

# Fast Database Generation for Parachute Cluster Design Using Navier-Stokes Equations on Supercomputers

G.P. Guruswamy\*

NASA Advanced Supercomputing Division  
 Ames Research Center, Moffett Field, CA, U.S.A.

## Abstract

**A fast procedure to simulate the unsteady aerodynamic characteristics of a parachute cluster in the vicinity of a capsule is presented. This problem is modeled using a well-validated flow solver, which solves the Reynolds-averaged Navier-Stokes equations for steady and unsteady compressible/incompressible flows about general geometries using an overset grid approach. Results are validated using comparisons with classical theory. The fast generation of a large aerodynamic database is accomplished using the dual-level parallel protocol on a massively parallel supercomputer.**

## I. Introduction

In order to advance human exploration of space, NASA is working on the Space Launch System (SLS), which utilizes a number of design concepts from the Apollo and Space Shuttle programs [1]. The new spacecraft will carry a crew exploration vehicle (CEV) known as Orion, which will accommodate up to six astronauts. A critical component in the design is the parachute deceleration system, which is required to ensure a safe landing of the capsule [2]. A photo of the Orion landing test without astronauts is shown in Fig.1

Parachutes, of course, were successfully used for all Apollo missions. However, as stated in Ref. 3, a major difficulty in design and development of these deceleration systems was the lack of adequate analytical methods to properly predict dynamic behavior, including loads and stresses on multiple parachute systems. These systems involve moving components in subsonic flow dominated by vortices and their complex interactions. Strong non-linear coupling occurs between the flow field and structural elements due to these large movements [3].

Accurate modeling of flows requires a solution of the unsteady Navier Stokes equations through the use of Computational Fluid Dynamics (CFD) that can efficiently model moving grids, including bodies with relative motion to each other. Use of such a tool is critical since the CEV capsule will have more payload than the Apollo capsule, and it may be required to land on the ground [1].

Since the Apollo program, computational methods for both fluids and structures have advanced significantly, particularly for fluids. However, design of a parachute system for the Orion capsule still utilizes the linear aerodynamic theory available in NASTRAN while modeling the multi-body dynamics using the ADAMS module [4].

Use of higher fidelity models for parachutes has already begun. Reference 5 presented computations on a flexible isolated canopy with capsule using the Euler equations. It included validation of pressures with the experiment. Reference 6 presented a finite-element approach to solve incompressible flows over flexible canopy clusters but did not include the capsule or any validation. It should be noted that compressibility effects are also important because of the flexibility of parachute canopies and their large relative movements. [7]

---

\*Sr. Scientist, Fundamental Modeling and Simulation Branch, AIAA Associate Fellow



Fig. 1. A snap-shot from a NASA experiment of Orion landing with parachutes.

A literature survey within the scope of this work reveals that the data to validate CFD for parachute systems are seldom available in the public domain. Most of the data available is in the form of global stability derivatives for a complete system without details such as surface pressures. The majority of previously published data using CFD has relied on the argument of self-consistent calculations and models [6]. In this paper, a well-validated CFD code for steady and unsteady flows including compressibility and incompressibility effects over complex configurations is selected. Grids are selected based on grid sensitivity studies. Results are validated with the linear theory.

At NASA, a variety of well-validated CFD codes that solve the Reynolds-Averaged Navier-Stokes (RANS) equations using the patched-structured (HiMAP) [8], overset-structured (OVERFLOW) [9], and unstructured (FUN3D) [10] grid approaches are routinely in use for flow computations about complex configurations. Accurate simulation of the CEV parachute-landing problem requires a CFD code—such as one of the codes listed above—with a robust moving grid capability. The OVERFLOW compressible/incompressible flow solver is well-validated for unsteady flows on flexible configurations [11] with a robust ability to model moving components [12]. Hence, it has been selected for the present study.

The design of a parachute system involves the evaluation of many parameters, which requires the development of a large aerodynamic database. However, evaluating a single configuration at a single design point can be computationally expensive (relatively speaking) due to flow field nonlinearities. Thus, the use of a large super cluster computer system, such as Pleiades at NASA Ames [13], with the ability to facilitate a dual-level parallel processing [14], is crucial for the fast generation of such a complex database.

In this paper, large-scale computations are made in the low subsonic regime for a typical parachute cluster system consisting of three semi-hemisphere canopies attached to a capsule based on Apollo module. It is noted that canopies of the Orion parachute system are based on spherical shapes and the module is based on the Apollo capsule. Grids are selected based on grid sensitivity studies. Results are validated with classical aerodynamic theory. The advanced parallel computing utility RUNDUA [14] is used for efficient use of massive parallel processing. The effects of the motions of the canopies and capsule on drag forces are studied. Results are demonstrated for generating large aerodynamic response surfaces (ARS).

## II. Results

In the present paper, the RANS equations [15] are numerically solved using the diagonal form of the Beam-Warming central difference algorithm [16], along with the one-equation Spalart-Allmaras turbulence model [17]. The solutions are computed using the OVERFLOW code [9], which utilizes an overset grid system. The second-order spatial and temporal accuracy options available in the 2.2h version of OVERFLOW are used throughout the present analysis. Dynamic motions are modeled using standard ‘xml’

input files [9]. OVERFLOW includes accurate modeling of incompressible flows using pre-conditioning [9].

### A. Steady State Computations on Isolated Canopy

Computations are first presented for an isolated semi-hemispherical canopy with and without a spill hole. The canopy is part of a sphere with the height to base-diameter ratio of 0.25. A body fitted near-body (NB) grid with C-O grid topology (C along radial direction and O in circumferential direction) is used to model the canopy with and without a spill hole of size 5% of canopy diameter (D). Figure 2 shows the portion of the grid around the canopy with a spill hole. The number of grid points along the circumferential direction for canopy with and without spill holes are 572 and 600, respectively. The number points in circumferential and normal directions are 121 and 78, respectively. Based on earlier grid sensitivity studies [18], a normal spacing of 0.000025D with a surface stretching factor of 1.125 is used. This yields a  $y^+$  value (one grid point away from the surface) that varies between 0.959 and 1.14, which is considered adequate to resolve flows at the surface. The spill hole is modeled using a cylindrical grid with 18 radial points, 156 axial points and 121 circumferential points. The outer boundaries are located about one diameter from the center. The direction of the flow is assumed to be in the positive direction of the x-axis.

In the present study, most computations are performed for free stream Mach numbers ( $M_\infty$ ) that vary from 0.1 to 0.3. (0.3 is the Mach number around which Orion's main parachutes are deployed). The Reynolds number ( $Re_D$ ) based on a assumed canopy of diameter of 2 ft (typical wind tunnel model) is  $2 \times 10^6$  for Mach number 0.2. The NB grid is embedded in the off-body (OB) grid system with the smallest spacing of 0.025D. The locations of outer boundaries for this OB grid system are selected based on grid sensitivity studies

The grid resolution is selected based on a grid sensitivity study performed for a canopy with spill hole at  $M_\infty = 0.2$ . Figure 3 shows that the residual of the canopy grid drops by 3 orders in 12000 iterations. Figure 4 shows a study comparing different outer boundary locations of the OB grid, and indicates that a location of the outer boundary at 10 canopy diameters is adequate. The remaining computations are made with the outer boundary at 15 diameters. This results in a grid of size 275x275x275 for the OB grid system. The resulting total number of grid points is 26.5 million.

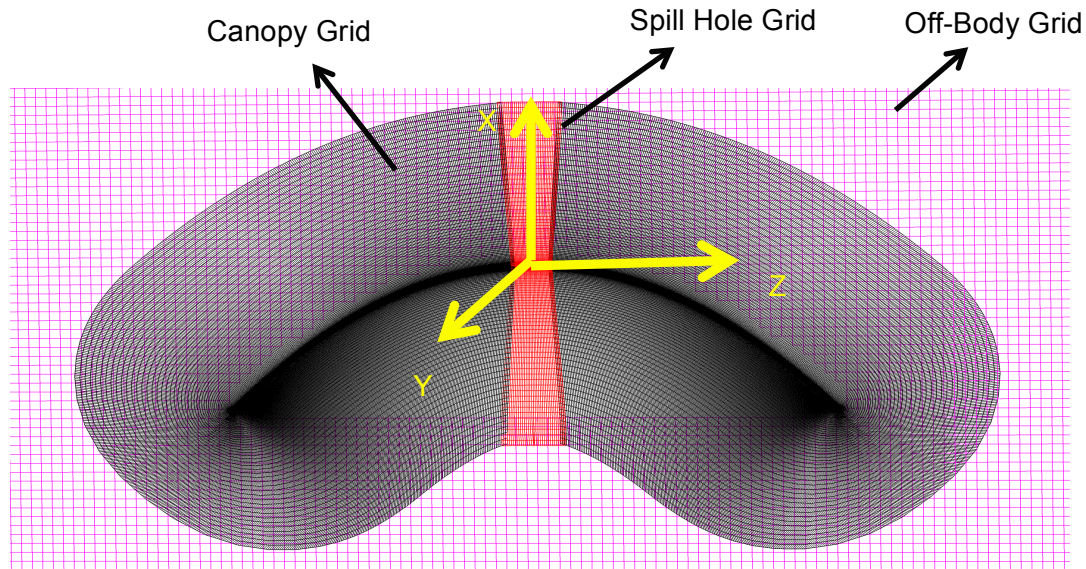


Fig. 2. Portion of near-body (NB) grid surrounding the isolated canopy with a spill hole.

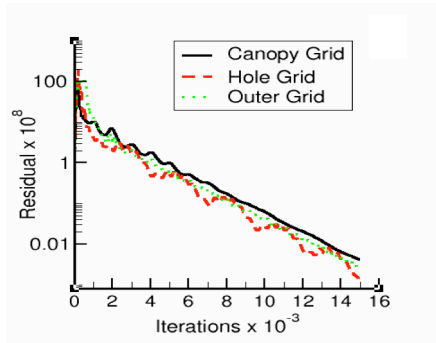


Fig. 3. Residual convergence at  $M_\infty = 0.20$ ,  $Re_D = 2$  million.

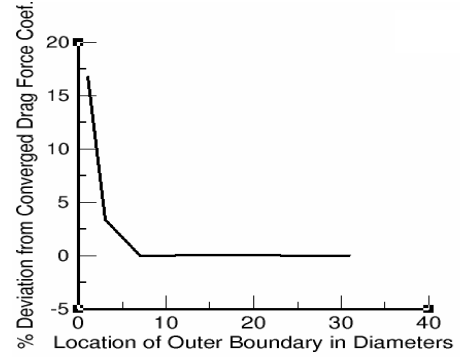


Fig. 4. Effect of outer boundary location on drag coefficient.

Figure 5 shows the distribution of inner surface coefficient of pressure ( $C_p$ ) along the radial direction (where  $R$  is the radius of the canopy) of canopies with and without a spill hole (also called canopy with a solid surface) in comparison with results from the vortex lattice based linear theory for a solid surface [19]. In general, computed results for solid surface canopy are about 6% lower, on average, than the linear theory and agree well in trend. For the case with a spill hole, inner surface  $C_p$  is lower than that for the solid canopy up to 80% the radius of canopy. The computed drag force coefficient  $C_d$  for the solid surface canopy is 1.36, which is in good agreement with the linear theory value of 1.38. It is noted that the linear theory does not provide more flow details than surface pressures. Navier-Stokes equations that model compressible flows are needed for detailed study of flows such as the effects of vortices on performance.

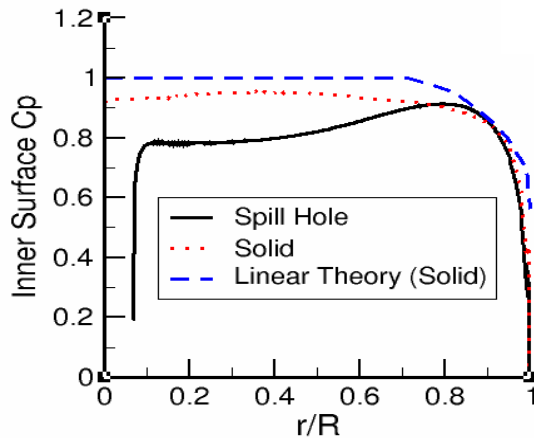


Fig. 5. Radial distributions of inner surface  $C_p$ , with and without spill hole, along with the linear theory at  $M_\infty = 0.20$ ,  $Re_D = 2$  million for a single canopy configuration.

Figure 6 shows carpet plots of Mach number distribution and inner surface  $C_p$  for canopies without (a) and with (b) spill hole at  $M_\infty = 0.20$ ,  $Re_D = 2$  million when the flow is converged to the steady-state results. The addition of the spill hole reduces the inner surface  $C_p$  and changes the flow pattern. The changes in flow pattern downstream of the canopy are more significant than upstream of canopy.

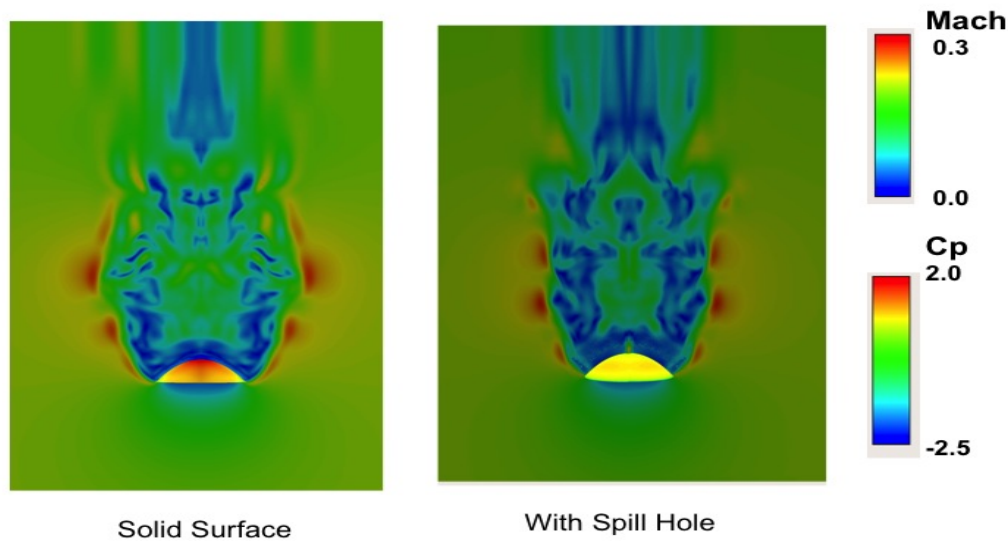


Fig. 6. Carpet plots of Mach number distribution and canopy inner surface  $C_p$  for canopies without (a) and with (b) spill hole at  $M_\infty = 0.20$ ,  $Re_D = 2$  million.

### B. Steady State Computations on Parachute Cluster

Having studied the flow field for an isolated canopy with a spill hole, a cluster of three parachute canopies with a typical capsule, shown in Fig. 7, is considered next. The capsule is selected from a test case in OVERFLOW code for an Apollo module. Positions of the canopies are initialized by rotating Canopy\_1 by 15 degrees in the X-Z plane, Canopy\_2 by -15 degrees in the X-Z plane then -15 degrees in the X-Y plane, and Canopy\_3 by 15 degrees in the X-Y plane using the 'Config.xml' input file of OVERFLOW. The radius of rotation is set to 2.0 diameters of the canopy. The grid for each canopy is from the study of the isolated canopy (see previous section). The spherical grid for the capsule is taken from the test cases of OVERFLOW code. It has 115 circumferential, 61 radial, and 79 normal grid points. The vertex of the capsule is located at 2 diameters from the vertices of the canopies. The cluster is embedded in the Cartesian off-body grid previously used for the isolated canopy, resulting a total grid size of 37.5 million points. A cross sectional view of the grid topology is shown in Fig. 8. The OVERFLOW code has a very efficient built-in procedure to combine the near body grids and off-body grid [9].

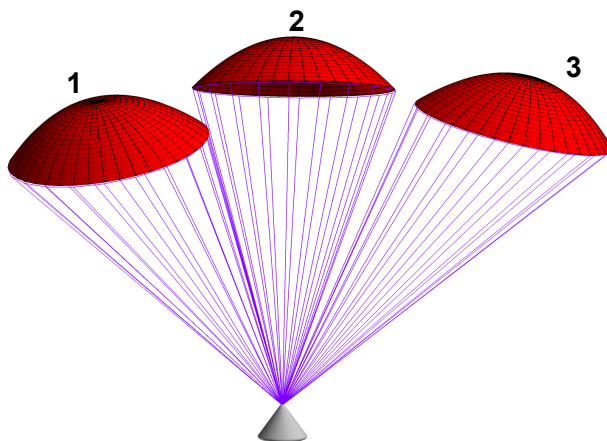


Fig. 7. A cluster of three canopies and a capsule used in this study.



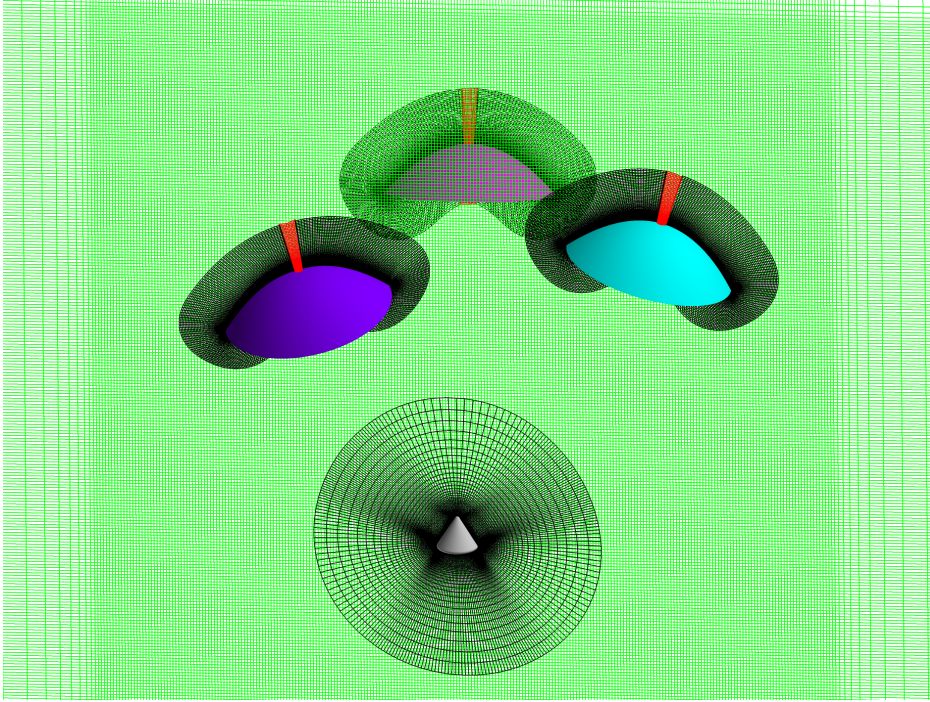


Fig. 8. A cross-sectional view of a 3D grid system used for this study.

Steady state computations are made at  $M_\infty = 0.2$  to study the convergence by using the variable time step option in OVERFLOW while the configuration is stationary. Figure 9 shows that in 12,000 iterations the residual for the canopy grids and the capsule grids drop by about 3 orders and 5 orders, respectively. Hence, all steady state computations used 12,000 iterations.

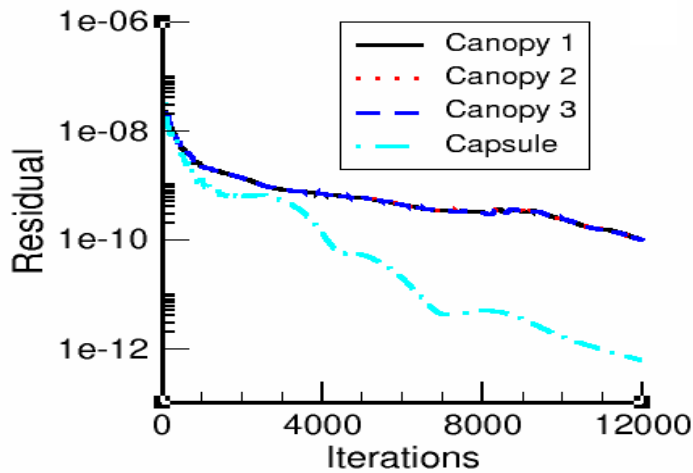


Fig. 9. Residual convergence for parachute cluster.

Figures 10a and 10b show the predominant inner surface  $C_p$  on canopies (plotted on outer surface to show in the same plot with external Mach number pattern), outer surface  $C_p$  on the capsule, and Mach number carpet plot for field sections through the center of Canopy\_2 and center of capsule and Canopy\_3. The effect of the spill hole can be seen on Mach contours.

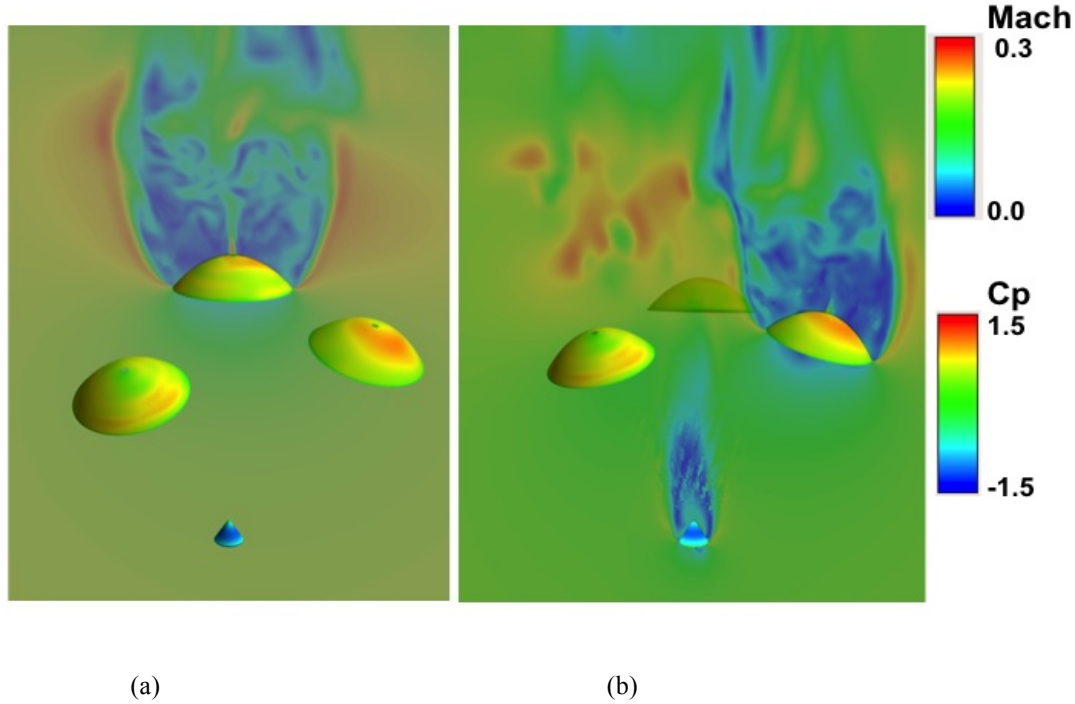


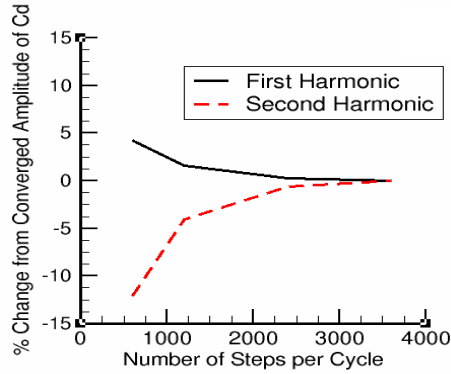
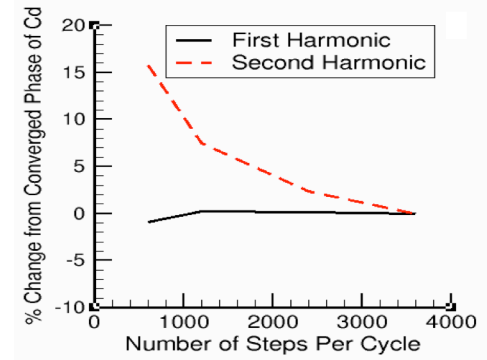
Fig. 10. Inner surface  $C_p$  on canopies, outer surface  $C_p$  on capsule, and Mach number carpet plot for field sections through a) center of second (rear) canopy and b) center of capsule and third canopy.

### C. Dynamic cases

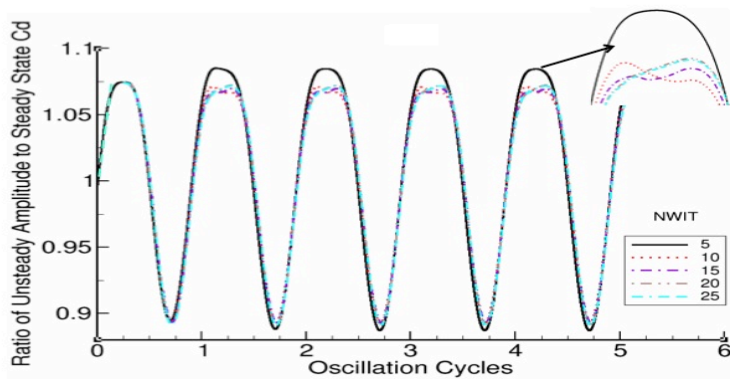
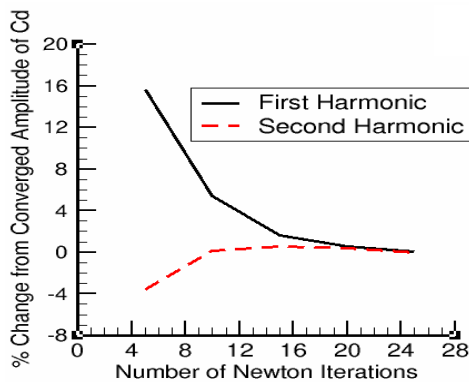
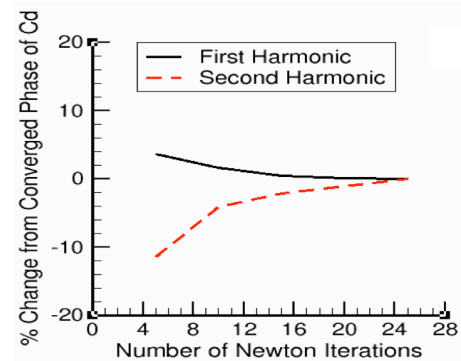
Next, the aerodynamic responses induced by multi-body dynamics of the parachute cluster are studied. OVERFLOW has extensive validated capabilities to time-accurately model moving rigid geometries [9], as well as flexible geometries such as rotor blades [21]. In this paper, unsteady aerodynamic responses of the parachute cluster with a capsule are computed for motions typically needed for design. The descent of the parachute system is modeled by reducing the free stream Mach number in small steps. Oscillatory motions of the parachute canopies and the capsule are modeled using a six-degree-of-freedom body dynamics capability (SIXDOF) available in OVERFLOW.

For unsteady computations, it is required to find the time step size (or number of steps per cycle [NSPC]) and the number of Newton iterations (NWIT) for stable and accurate results. Newton sub-iterations are required to maintain 2<sup>nd</sup> order time accuracy. Computations are performed on the isolated canopy at  $M_\infty = 0.20$  to determine values for NWIT and NSPC. The canopy is prescribed to oscillate in radial plane (X-Z shown in Fig. 1) with an amplitude of 5 degrees at a rate of one cycle per second. First a minimum NSPC (maximum time step size) is determined by setting NWIT = 5.

Based on the Fourier analysis of responses, it is found that responses reached periodicity in two cycles. Results are extracted using the third cycle responses for NSPC equal to 600, 1200, 2400, and 3600. Figure 11 shows plots of percentage changes in amplitude of the first and second harmonics of  $C_d$  from the corresponding amplitudes of  $C_d$  at NSPC = 3600. The second harmonic amplitude of  $C_d$  is an order of magnitude smaller than that for the first harmonic amplitude. Similar plots for phase angle are shown in Fig. 12. Based on the first harmonic components in Figs. 11 and 12, NSPC = 3600 is found to be adequate for stable responses.

Fig. 11. Effect of NSPC on amplitude of  $C_d$ .Fig. 12. Effect of NSPC on phase of  $C_d$ .

The next computations are performed by increasing the NWIT in increments of 5 for NSPC = 3600. Figure 13 shows responses for NWIT = 5, 10, 15, 20 and 25. The solutions for cycles 2-4 are periodic. Results are extracted from the third cycle. Figure 14 shows plots of percentage changes in amplitude of the first and second harmonics of  $C_d$  from the corresponding amplitude of  $C_d$  at NWIT = 25. The amplitude of the second harmonic of  $C_d$  is an order of magnitude smaller than that for the first harmonic. Similar plots for phase angle are shown in Fig. 15. Based on the first harmonics in Figs 14 and 15, NSPC = 3600 and NWIT = 25 are found to be adequate for stable and accurate responses.

Fig. 13. Responses of  $C_d$  for various NWIT at NSPC = 3600.Fig. 14. Effect of NWIT on amplitude of  $C_d$ .Fig. 15. Effect of NWIT on phase of  $C_d$ .



As stated earlier, the data suitable to validate CFD are seldom available in public domain for parachute systems. Here, self-consistency of results is first established by performing grid sensitivity studies described above. In addition, validation is also accomplished by independently computing steady and unsteady responses using variable time step (non-time accurate) and constant time step (time-accurate) simulations for a rigid configuration. Starting each case from the free stream conditions, computations are made for a series of Mach numbers decreasing from 0.3 to 0.1. For time accurate computations, a time step corresponding  $NSPC = 3600$  and  $NWIT = 25$  is used. For convergence, time accurate computations required 1,200 global steps (total 30,000 steps including 25 Newton Sub-iterations) compared to 12,000 steps required for non-time accurate computations.

As seen from Fig. 16 (x-axis labels are in decreasing order to reflect descent motion), the unsteady results are close to steady results for Mach numbers between 0.3 and  $\sim 0.18$ , then deviates slightly as the Mach number is reduced further. The comparison of time accurate results with validated steady state results provides the confidence to perform time accurate computations for the cluster of parachutes.

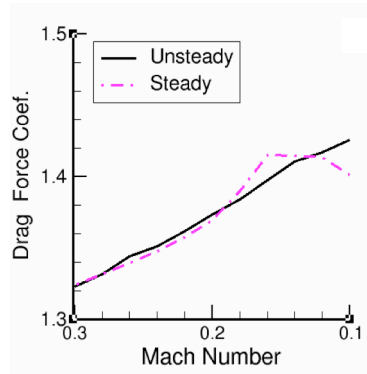


Fig. 16. Steady and unsteady  $C_d$  during the descent.

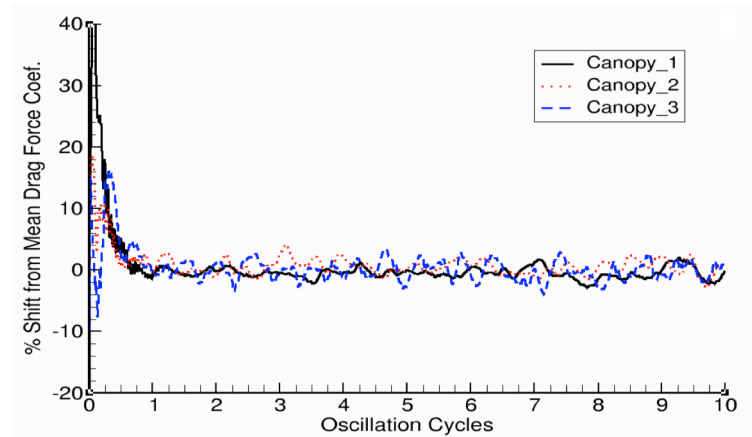


Fig. 17.  $C_d$  time responses of Canopies in cluster.

Next, time accurate computations are demonstrated for the parachute cluster. Using the SIXDOF option of OVERFLOW, all canopies and the capsule are prescribed to oscillate about their own X-Z planes with 5 degrees amplitude and a frequency of 1 Hz, while the whole system is descending at a non-dimensional velocity of 0.002. Computations are made at instantaneous  $M_\infty = 0.2$  by setting NSPC and NWIT to 3600 and 25, respectively, based on computations on the isolated canopy. Figure 17 shows the percentage shifts of time responses of  $C_d$  of three canopies (see Fig. 8), with respect to their respective mean  $C_d$ , for 10 cycles of oscillation. For all three canopies, responses are transient and contain higher harmonics. Amplitude of oscillations for Canopy\_1 is smaller than other two canopies.

Figure 18 shows a typical snapshot of vorticity magnitude contours during descent for the three-canopy parachute and capsule configuration at a Mach number of  $\sim 0.3$ . The canopies and capsule are all oscillating.

### III. Parallel computing

One of the main purposes of this paper is to demonstrate the fast computation of a large database. In Ref. 14, a parallel protocol called RUNDUA was developed, which creates an efficient single-job computing environment for multiple cases. If enough processors are used, the resulting wall-clock time for a typical multiple case calculation series is nearly the same as a single case.

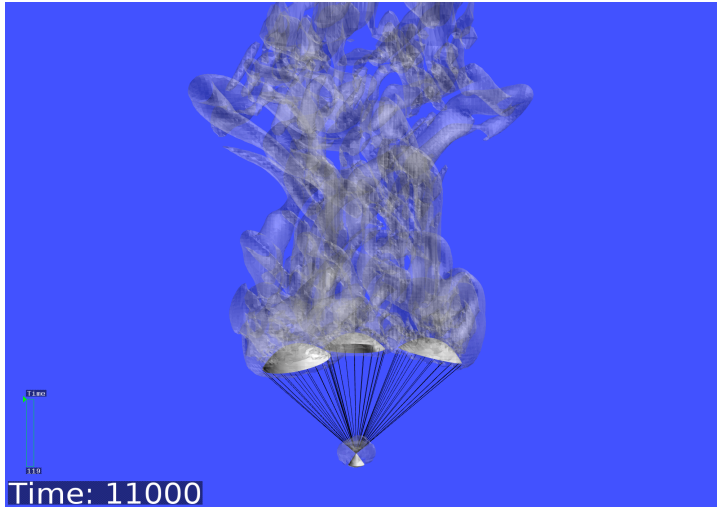


Fig. 18. Snapshot showing iso-surfaces of vorticity magnitude during descent at  $M_\infty = 0.30$  for the three-canopy parachute and capsule configuration.

The present approach is aimed towards generating aerodynamic response surfaces for possible deformations of a parachute system. A similar approach to compute aerodynamic influence coefficients for a rotor system is reported in Ref. 21. By using a linear combination of individual responses, aerodynamic forces for any arbitrary displacement can then be computed. The following approach is taken to compute the ARS matrix using OVERFLOW code:

1. Deformation pattern such as variation of coning angle in selected.
2. A set of 'Configuration.xml' files that input deformations to OVERFLOW are created.
3. Inputs for different cases with varying Mach numbers are generated. It is assumed the number of iterations specified is adequate for convergence for all cases.
4. Data is spawned to different directories, which are contiguously numbered.
5. All cases are computed, running each case on a different group of cores using 'Rank' identification [14].
6. Successful completion of all jobs can be tracked by monitoring the size of the residual files. Once a Parallel Batch System (PBS) job is successfully completed, all residual files will be of the same size. It is assumed that the user has selected appropriate parameters so that results converge at the end of the job completion.
7. After all jobs are successfully completed, data, such as drag, is extracted.

Figure 19 shows flow diagram of RUNDUA.

### A. Isolated Canopy

First results are demonstrated for the isolated canopy with a spill hole. The generation of a database consisting of computed results for 10 Mach numbers, ranging from 0.3 to 0.12 in decrements of 0.02, and 10 angles of attack ranging from 0.0 deg to 4.5 deg in increments of 0.5 deg (a total of 100 individual cases each, with 26.5 million grid points) is now described. All cases were run using RUNDUA as a single job on the Pleiades supercomputing system [22]. Each individual case was assigned to 40 cores and was run for 12,000 iterations. Using 4,000 cores, all 100 cases were completed in a wall-clock time of 4.61 hrs, 1.8% more time than was required to run a single case in a stand-alone method. Figure 21 shows a carpet plot of drag coefficients for all 100 cases. In general, drag increases with a decrease in Mach number similar to observations made in the wind tunnel test [23]. With increasing angle of attack, drag first increases, then drops for all Mach numbers.

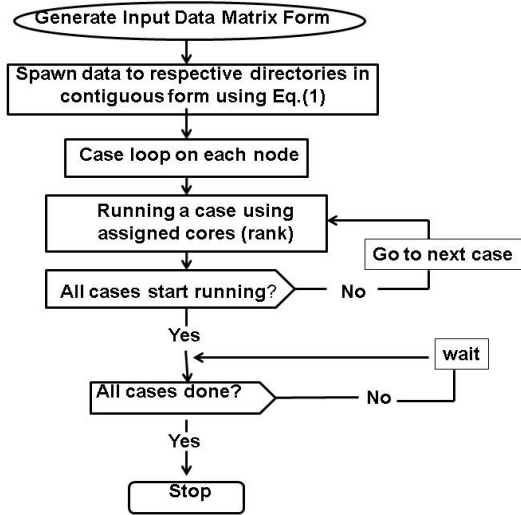


Fig. 19. Flow diagram of RUNDUA (Ref. 14).

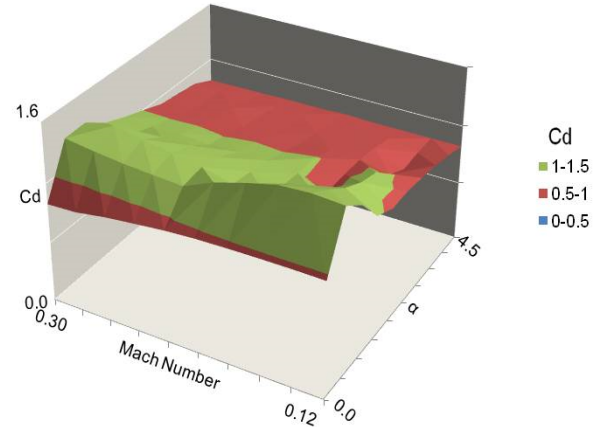


Fig. 20. A100-case demonstration for the isolated canopy using RUNDUA.

## B. Parachute Cluster

The next results are demonstrated for the parachute cluster shown in Fig. 7. For this case, 5 Mach numbers ranging from 0.3 to 0.1 in decrements of 0.05, and 5 coning angles (in X-Z plane) ranging from 15 deg. to 19 deg. in increments of 1 deg. were selected. These 25 cases were run in a single job environment with 160 cores assigned to each case, resulting in a request for a total of 4,000 cores. All 25 cases, with 37.5 million grid points each, were run for 12,000 iterations, during which the residuals dropped by about 3 orders. The total wall-clock time required for all 25 cases was 2.21 hrs., about 2% more than that required for a single case in a single job.

Figure 21 shows plots of  $C_d$  for decreasing Mach number with coning angles increasing from 15 to 19 degrees. Drag forces increase with the decrease in Mach number for coning angles at 15 and 16 degrees. For angles larger than 17 degrees,  $C_d$  slightly decreases with the decrease in Mach number. For any given Mach number,  $C_d$  decreases with an increase in coning angle. This can be attributed to the effective area of the canopy, which contributes to drag decrease with an increase in coning angle.

## VI. Conclusions

To date, other than the linear theories, mostly the Euler equation-based incompressible flow solvers are in use for simulating parachute clusters. In this study, a more advanced Reynolds Averaged Navier-Stokes equation-based, high fidelity procedure valid for both compressible and incompressible flows is presented, including modeling of a canopy. Flow modeling includes the viscous and compressibility/ incompressibility effects needed to model the configuration, contrary to the use of incompressible and inviscid flow solvers in previous work. Computed results show good comparison with the linear theory. Using the state-of-the-art parallel computing protocol, a computation for 100 cases of isolated canopy (each with 26.5 million grid points) is completed in a single job that requires only about 4.5 hours of wall-clock time with the use of 4,000 cores. Using the same number of cores, 25 cases were completed in 2.2 hours of wall-clock time for the parachute cluster modeled using 37.5 million grid points. Motions with oscillating canopy and capsule are demonstrated using the time accurate computations. Future work involves adding flexibility for canopies and aeroelastic computations.

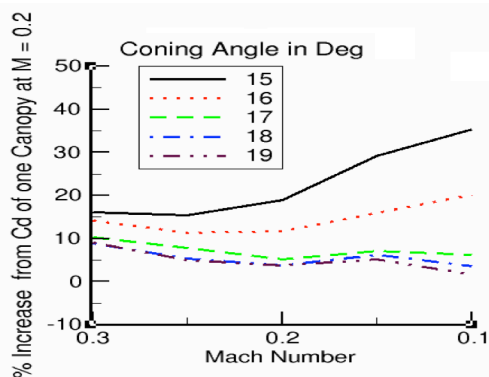


Fig. 21. Effect of Mach number and coning angle on the drag force coefficient.

### Acknowledgements

The author would like to thank Pieter Buning of NASA Langley Research Center and William Chan of NASA Ames Research Center (ARC) for providing consultations in multi-body motion capability associated with the OVERFLOW flow solver. Discussions with Shishir Pandya of ARC on grid topology were helpful. Help with animation by Tim Sandstrom and parallel computing by David Barker of the NASA Advanced Supercomputing Division are appreciated.

### References

1. "NASA's Exploration Systems Architecture Study," NASA TM-2005-214062, Nov. 2005.
2. Marshall, P. and Norris, S. D., "Orion Program Status," AIAA Space 2013 Conference and Exhibition, AIAA 2013-5476, San Diego, CA, Sept. 2013.
3. Knacke, T. W., "The Apollo Parachute Landing System," TP-131, North American Rockwell and Northrop, Ventura, CA, Sept. 1968.
4. Moore, J. W. and Romero, L. M., "An Airborne Parachute Compartment Test Bed for the Orion Parachute Test Program," AIAA 2013-1289, AIAA Aerodynamic Decelerator Systems (ADS) Conference, March 2013, Daytona Beach, FL.
5. Guruswamy, G.P. "Euler/Navier-Stokes Based Unsteady Aerodynamics and Aeroelasticity of a Capsule Landing System," AIAA-2007-2063, 48th AIAA Structural Dynamics Conference, Honolulu, Hawaii, April 2007.
6. Takizawa, K., Wright, S., Moorman, C. and Tezduyar, T. E. "Fluid-Structures Interaction Modeling of Parachute Clusters," *International J. for Numerical Methods in Fluids*, Vol. 65, May 2011, pp. 286-307.
7. Kumar, V., "Advanced Computational Techniques for Incompressible/ Compressible Fluid-Structure Interactions," PhD Thesis, Rice University, Houston Texas, April 2005.
8. Guruswamy, G. P., Byun, C., Potsdam, M and Farhangnia, M., "User's Manual for HiMAP - A Multilevel Parallel Multidisciplinary Analysis Process," NASA TM-1999-209578, Sept. 1999.
9. Nichols, R. H., Tramel R. W. and Buning P. G., "Solver and Turbulence Model Upgrades to OVERFLOW2 for Unsteady and High-Speed Applications," AIAA Paper 2006-2824, AIAA 36th Fluid Dynamics Conference, San Francisco, CA, June 2006.
10. Biedron, R. T., Vatsa, V. and Atkins, H. L., "Simulation of Unsteady Flows Using an Unstructured Navier-Stokes Solver on Moving and Stationary Grids," AIAA-2005-5093, Applied Aerodynamics Conference, Toronto, Canada, June 2005.
11. Guruswamy, G.P., "Computational-Fluid-Dynamics and Computational-Structural-Dynamics Based Time-Accurate Aeroelasticity of Helicopter Blades," *J. of Aircraft*, Vol. 47, No. 3, May-June 2010, pp. 858-863.
12. Flora, T. J. and Johnson, R., "Comparison of Experiments and OVERFLOW Modeling of Store Release from a Cavity at Mach 3," Overset Symposium, Oct. 2012, Dayton, Ohio.

13. Guruswamy, G.P., "Large-Scale Computations for Stability Analysis of Launch Vehicles Using Cluster Computers," *J. of Spacecraft and Rockets*, Vol. 48, No. 4, July-August 2011, pp. 584-588.
14. Guruswamy, G.P., "Dual Level Parallel Computations for Large Scale High-Fidelity Database to Design Aerospace Vehicles," *NASA/TM-2013-216602*, Sept. 2013.
15. Peyret, R. and Viviand, H., "Computation of Viscous Compressible Flows based on Navier-Stokes Equations," AGARD-AG-212, 1975.
16. Pulliam, T. H. and Chaussee, D. S., "A Diagonal Form of an Implicit Approximate-Factorization Algorithm," *J. of Computational Physics*, Vol. 39, No. 2, 1981, pp. 347-363.
17. Spalart, P. R., "Direct Simulation of a Turbulent Boundary Layer," *J. of Fluid Mechanics*, Cambridge University Press, 1988, 187, pp. 61-98.
18. Guruswamy, G.P., "A Modular Approach to Model Oscillating Control Surface using Navier-Stokes Equations," 5th Decennial AHS Aeromechanics' Specialists Conf., San Francisco, Jan. 2014.
19. Klimas, P. C., "Fluid Mass Associated with an Axi-symmetric Parachute Canopy," *J. of Aircraft*, Vol. 14, No. 6, June 1977, pp. 577-580.
20. Guruswamy, G.P., "Time-Accurate Aeroelastic Computations of a Full Helicopter Model using the Navier-Stokes Equations," *International J. of Aerospace Innovations*, Vol. 5, No 3+4, Dec 2013, pp. 73-82.
21. Guruswamy, G.P., "Frequency Domain Flutter Boundary Computations Using Navier- Stokes Equations on Superclusters," *J. of Aircraft*, Vol. 51, No. 5, Sept-Oct 2014.
22. Mehrotra, P., Pryor, L. H., Bailey, F. R, and Cotnoir, M., "Supporting 'Big Data' Analysis and Analytics at the NASA advanced Supercomputing (NAS) Facility," NAS Technical Report NAS-2014-02, January 2014, NASA Ames Research Center, Moffett Field, CA
23. Maydew, R. C., Peterson C. W, and Orik-Ruekemann, K. J, "Design and Testing of High Performance Parachutes," AGARD-AG-319, Nov. 1991.